

## Metaheuristic-optimized machine learning models for predicting the unconfined compressive strength of geopolymer-stabilized clay soils

Khadije Mahmoodi<sup>1\*</sup> and Seyed-Amir Banimahd<sup>1</sup>

<sup>1</sup> Assistant Professor, Department of Civil Engineering, Faculty of Engineering, Ardakan University, Ardakan, Iran

(Received: 18 November 2025, Accepted: 21 February 2026)

### Abstract

The low strength of clay soils is one of the main challenges in road construction projects. Geopolymerization using various additives such as fly ash, blast furnace slag, and alkaline activators is a common method to improve the mechanical properties of these soils. However, accurate and rapid evaluation of the effects of these materials on soil strength traditionally requires extensive and time-consuming laboratory tests. This study proposes an integrated machine-learning framework to predict the unconfined compressive strength (UCS) of clay soils stabilized with fly ash and blast-furnace slag. A dataset comprising 283 experimental samples of lime/slag-stabilized clay activated with sodium hydroxide was utilized. Input variables include fly ash and slag percentages, alkaline activator molarity, alkaline-to-binder ratio, atomic Na/Al and Si/Al ratios, and the soil's liquid and plastic limits. To this end, several machine learning models including artificial neural networks (ANN), support vector machines (SVM), decision trees (DT), and extreme gradient boosting (XGBoost), were employed in combination with metaheuristic optimization algorithms such as ant colony optimization (ACO), particle swarm optimization (PSO), and genetic algorithm (GA). The findings revealed that the proposed ANN-PSO hybrid model demonstrated outstanding predictive accuracy, achieving an  $R^2$  value of 0.98, confirming its effectiveness for reliable UCS estimation. Sensitivity analysis further indicated that blast furnace slag was the most influential factor in enhancing soil strength, while the type of clay also had a considerable effect on the final UCS.

**Keywords:** Blast furnace slag, geopolymer-stabilized clay soil, machine learning prediction, metaheuristic optimization algorithms

---

\*Corresponding author:

mahmoodi@ardakan.ac.ir

## 1 Introduction

The presence of low-strength clayey soils in the roadbeds is one of the most important factors affecting the stability and durability of pavements. Non-uniform settlements, premature pavement failure, and increased maintenance costs are among the problems caused by the use of these types of soils in road construction projects. Various methods, such as stabilization with cement and lime, are used to improve the engineering characteristics of clayey soils. However, these methods are associated with environmental challenges due to high energy consumption and greenhouse gas production. In contrast, geopolymerization technology, as a green and sustainable method, has great potential to improve the mechanical properties of clayey soils and increase the useful life of pavements (Hoy et al., 2016). In the geopolymerization process, by creating a reaction between pozzolanic materials and alkaline activators, silicate gels are formed, which cause the adhesion of soil particles and increase its resistance to stresses. In addition to environmental benefits, soil geopolymerization also competes with traditional stabilization methods in terms of mechanical properties (Behnood, 2018; Ghadir and Ranjbar, 2018).

Previous research has shown that the use of activators can significantly improve the mechanical properties of clay soils during the soil stabilization process. Miao et al. (2017) used potassium hydroxide and calcium hydroxide as activators to stabilize clay. The results showed that during the stabilization process, the swelling percentage and plasticity index of the soil decreased, and the uniaxial compressive strength (UCS) of the soil

increased. Sukprasert et al. (2021) investigated the mechanical properties of silty clay stabilized with volcanic ash and blast furnace slag. They investigated the effect of replacing ash with slag, alkaline activator concentration, and curing time. The results showed that the use of sodium hydroxide activator causes the release of silicates and aluminates from volcanic ash and the formation of more cement gel, which in turn increases the efficiency of the soil stabilization process. Evaluating the efficiency of different stabilizers and assessing the influence of curing conditions such as temperature, humidity, curing age, and the presence of activators, require extensive laboratory testing, which is both time-consuming and costly. In recent years, with the advancement of artificial intelligence, various machine learning methods have been used to estimate many mechanical properties of various materials, including soil and concrete. Johari et al. (2011) employed artificial neural networks (ANNs) to generate stress–path curves for compacted unsaturated granular soils, demonstrating high accuracy in capturing the effects of dry density, stress state, and degree of saturation. Das et al. (2011) estimated the compressive strength and maximum dry density using backpropagation artificial neural network (BP-ANN) and support vector regression (SVR) algorithms, considering parameters such as sand, gravel, and clay percentage, liquid limit, moisture percentage, and cement content. Their study showed that SVR has higher accuracy in estimating the target parameter. Güllü (2014) estimated Young's modulus and compressive strength of stabilized soil using genetic algorithm and nonlinear regression. Mozumder et al. (2017) used the SVR

algorithm to estimate the UCS of blast furnace slag (GGBS) stabilized clay. The results showed that this method is efficient for estimating the strength of the stabilized soil. Heidari and Ghanizadeh (2020) used different artificial neural network (ANN) and adaptive neuro-fuzzy inference system (ANFIS) methods to estimate the compressive and tensile strengths of cement-stabilized clay and iron ore waste. The results showed that ANFIS has the best performance in estimating the model parameters and the cement percentage has the greatest effect in estimating the target parameters. Zhang et al. (2021) developed a hybrid machine learning model that includes extreme gradient boosting (XGBoost) and random forest (RF). This model was used to predict the undrained shear strength of soft clay soils. This study showed that the XGBoost and RF models have high efficiency in estimating the shear strength of soil with  $R^2 = 0.966$ . Johari et al. (2021) developed gene expression programming (GEP) models to estimate the collapsibility index of soils, achieving strong predictive performance, and extended this approach in 2022 to predict strain in nano-silica-stabilized soils. Ghanizadeh et al. (2022) estimated the UCS and modulus of elasticity (E) of lime and cement stabilized clay using evolutionary polynomial regression. The results showed that the percentage of cement and moisture content were the most effective parameters in estimating the UCS for cement and lime stabilized soil, respectively. Ghanizadeh and Naserlavi (2023) estimated the UCS and E of iron ore and lime-stabilized clay using Gaussian regression. The results showed that in the case of UCS, the percentage of moisture, curing time, percentage of

lime, and percentage of iron ore waste were the most effective parameters, respectively, and in the case of E, the percentage of moisture, percentage of lime, percentage of iron ore waste, and curing time were the most effective parameters, respectively. Mahmoodi and Momeni (2024) estimated the UCS of soil using various machine learning models including linear regression (LR), ANN, k-nearest neighbor (KNN), SVR, decision tree (DT), RF, and gradient boosting (GB). Grid search method was used to adjust the hyperparameters of the models, and 10-fold cross-validation (k-folds) method was used to increase the accuracy of the estimation. The evaluation results showed that the SVR and ANN models performed very well in estimating the UCS of the studied soil. In addition, sensitivity analysis showed that the characteristics of pozzolan percentage, alkaline activator molarity, and curing time have the greatest impact on the target variable (UCS). In another study, Mahmoodi et al. (2024) estimated the shear strength of lime-stabilized and geosynthetic-reinforced soil using ANN and SVM algorithms. The input characteristics of the models included lime percentage, type of reinforcement (different types of geogrids and geotextile), curing time, overburden pressure and moisture percentage. The results showed that among these characteristics, lime percentage and then type of reinforcement had the greatest effect on obtaining soil shear strength. Also,  $R^2$  values greater than 0.98 indicated high efficiency of the algorithms used in estimating the shear strength of the studied soil. Ghanizadeh et al. (2024) investigated UCS prediction of cement-stabilized iron ore tailings using various ML models, identifying ANN as the most accurate approach.

Ghanizadeh and Jahanshahi (2024) applied GEP to cement- and lime-stabilized clays, highlighting cement content and moisture as dominant factors. More recently, Ghanizadeh et al. (2025) employed multivariate adaptive regression splines (MARS) to predict UCS and CBR of lime-stabilized soils activated with rice husk ash, achieving excellent predictive accuracy. Abdullah et al. (2024) estimated UCS of stabilized soils using combined models of gradient boosting (GB) and adaptive boosting (AdaBoost). Sensitivity analysis showed that blast furnace slag content is the most important parameter affecting UCS.

Given the growing interest in machine learning for UCS prediction, this study addresses key limitations of previous research by developing an integrated framework that combines advanced learning models with population-based optimization algorithms for geopolymer-stabilized clay soils. Unlike earlier studies that primarily employed single models or conventional tuning methods, the proposed approach systematically couples ANN, SVM, DT, and XGBoost with ACO, PSO, and GA to enhance predictive accuracy and generalization. Using a comprehensive dataset of 283 experimental samples and incorporating detailed chemical and geotechnical parameters, this study provides a robust, efficient, and reliable tool for rapid UCS estimation. Furthermore, sensitivity and parametric analyses are conducted to identify the dominant factors influencing strength development, thereby offering practical guidance for sustainable pavement design and soil stabilization practice.

## 2 Materials and Methods

In this study, the methodology was developed to evaluate and predict the

unconfined compressive strength (UCS) of geopolymer-stabilized clay soils using advanced machine learning and optimization techniques. Experimental data were obtained from the study of Mozumder and Laskar (2015), which investigated the strength behavior of clayey soils stabilized with fly ash and blast furnace slag activated by sodium hydroxide under varying curing conditions. ML models, including XGBoost, ANN, SVM, and Decision Tree, were trained and optimized using metaheuristic algorithms such as ACO, PSO, and GA to achieve accurate and reliable UCS predictions. Figure 1 presents an overview of the study methodology, illustrating the integration of machine learning with metaheuristic algorithms for parameter optimization. This visual summary emphasizes the key stages involved in data collection, model training, and validation within the research process.

### 2.1 Material Properties and Data

The experimental dataset was originally generated to investigate the influence of soil type, additive content, and activator concentration on the UCS of stabilized clays (Mozumder and Laskar, 2015). Three types of clay with distinct geotechnical characteristics were used, as summarized in Table 1. These clays were stabilized using fly ash (FA), blast furnace slag (S), and sodium hydroxide (NaOH) as the alkaline activator.

**Table 1.** Characteristics of the clay used (Mozumder and Laskar, 2015).

Soil Type	Soil Classification	LL (%)	PL (%)	PI (%)	$\gamma_{dmax}$ ( $kN/m^3$ )
S1	CH	116	28	88	14.0
S2	CH	52	26	26	15.0
S3	CL	38	24	14	16.5

Kiln-dried clay was thoroughly mixed with the stabilizing materials to ensure uniformity. The proportion of stabilizer varied between 4–50% for slag (S), 4–20% for fly ash (FA), and 4–50% for their combined mixtures. The molarity of the alkaline activator (M) ranged from 4 to 14.5 mol/L, and the alkaline-to-binder ratio (A/B) was set to 0.45, 0.65,

and 0.85. Na/Al and Si/Al are also the atomic ratio of Na to Al and Si to Al of the mixture, respectively. The prepared samples were cured for 28 days under ambient conditions and subsequently immersed in water before UCS testing. The statistical characteristics of the dataset are presented in Table 2.

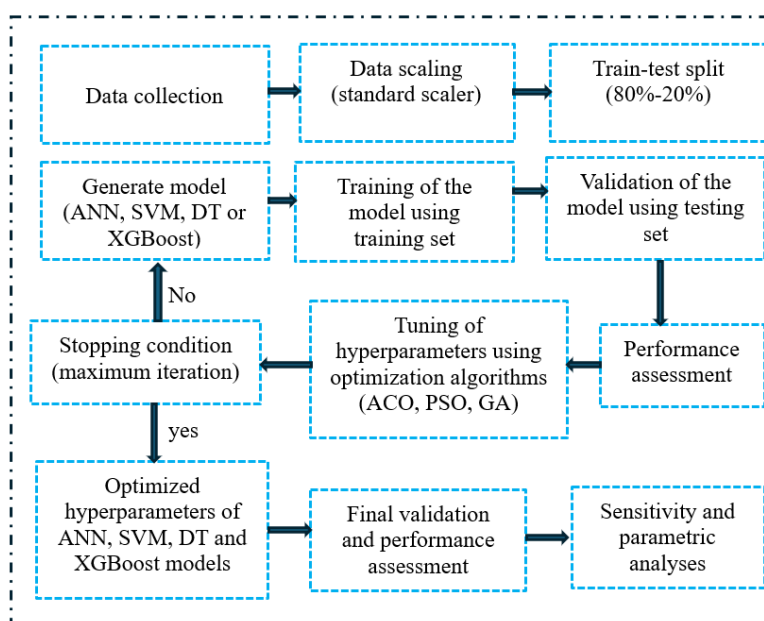


**Figure 1:** The methodology diagram of the study.

**Table 2.** Statistical characteristics of the data set (Mozamder and Laskar, 2015).

Property	Mean	Minimum	Maximum	Standard Deviation
LL	62.6	32.2	116.0	31.6
PI	37.8	14.1	88.5	30.1
S (%)	16.0	0.0	50.0	13.1
FA (%)	2.2	0.0	20.0	4.8
M (%)	12.5	2.7	15.0	2.6
A/B	0.6	0.1	0.9	0.1
Na/Al	1.2	0.2	2.0	0.4
Si/Al	1.7	0.3	2.5	0.4
UCS (MPa)	5.9	0.0	24.3	6.6

## 2.2 Machine Learning Algorithms

Machine learning (ML) algorithms are powerful data-driven tools for extracting meaningful patterns from existing

datasets. One of the main categories of ML is supervised learning, in which each training instance is associated with a known response variable. Using this information, the algorithm learns the underlying relationships between input features and output parameters. In this study, four supervised ML algorithms—artificial neural network (ANN), support vector regression (SVR), decision tree (DT), and extreme gradient boosting (XGBoost)—were employed to estimate the unconfined compressive strength (UCS) of stabilized soils.

### 2.2.1 Artificial neural network (ANN)

Artificial neural networks (ANNs) are computational models inspired by the

human brain, designed to model complex nonlinear dependencies in large datasets. They are widely used in supervised learning tasks such as classification and regression due to their strong approximation capability. An ANN consists of interconnected processing units (neurons) arranged in input, hidden, and output layers. During training, connection weights are iteratively updated via the backpropagation algorithm to minimize the difference between predicted and actual outputs. For each neuron, the input data are multiplied by corresponding weights, summed with a bias term, and passed through an activation function (Eq. 1) to produce an output (Theobald, 2017):

$$y = f\left(\sum_{i=1}^n w_i x_i + b\right) \quad (1)$$

where  $x_i$  is the input,  $w_i$  is the connection weight,  $b$  is the bias term, and  $f$  is the activation function.

### 2.2.2 Support Vector regression (SVR)

Support Vector Regression (SVR) extends the framework of Support Vector Machine (SVM) to the task of predicting continuous variables. The main goal of SVR is to identify a regression function ( $f(x)$ ) that effectively captures the relationship between input and output variables while minimizing the prediction error and model complexity. This is achieved by constructing an optimal hyperplane. The data points that lie outside this region, known as support vectors, play an important role in defining the regression function. The optimization process involves minimizing a regularized risk function that balances the smoothness of the model and the empirical error. By using kernel functions (such as linear,

polynomial, or radial basis functions), SVR can effectively model nonlinear relationships in high-dimensional feature spaces, thereby providing accurate and generalizable regression performance. The optimization objective is defined in Eq. (2) and minimized subject to the constraints in Eqs. (3) and (4) (Zhou et al., 2014):

$$\frac{1}{2} \|w\|^2 + C \sum_{i=1}^l (\xi_i + \xi_i^*) \quad (2)$$

where

$$\begin{cases} y_i - \sum_{j=1}^n \sum_{i=1}^l w_j x_{ji} - b \leq \varepsilon + \xi_i \\ \sum_{j=1}^n \sum_{i=1}^l w_j x_{ji} + b - y_i \leq \varepsilon + \xi_i^* \\ \xi_i, \xi_i^* \geq 0 \end{cases} \quad (3)$$

and

$$f(x) = \sum_{j=1}^n w_j x_j + b, \quad (4)$$

$$w \in R^n, b \in R$$

In these relations,  $n$  is the number of features,  $b$  is the bias value, and  $w$  is the weighting variable. The parameter  $C$  also balances the complexity of the function  $f$  and the acceptable error rate. In the SVR algorithm, errors less than  $\varepsilon$  are allowed. However, if the error exceeds  $\varepsilon$ , penalties are applied by the variables  $\xi_i$  and  $\xi_i^*$ .

### 2.2.3 Decision Tree (DT)

A Decision Tree (DT) recursively partitions the feature space into subsets based on decision rules derived from input variables. Each internal node represents a feature, each branch a decision rule, and each leaf node an output value. Its simplicity, interpretability, and ability to handle nonlinear relationships make it a popular choice for regression problems. To

prevent overfitting, pruning techniques are typically applied (Raschka et al., 2022).

### 2.2.4 Extreme Gradient Boosting (XGBoost)

Extreme Gradient Boosting (XGBoost) is an ensemble algorithm that builds a series of decision trees sequentially, where each new tree attempts to correct the errors of the previous ones. This iterative process improves model accuracy and robustness. The objective function of XGBoost is defined as follows (Dhaliwal et al., 2018):

$$Obj(\theta) = \sum_{i=1}^n L(y_i, \hat{y}_i) + \sum_{k=1}^K \Omega(f_k) \quad (5)$$

where  $n$  denotes the number of training samples,  $k$  represents the number of decision trees,  $y_i$  is the actual value, and  $\hat{y}_i$  is the predicted value.  $L(y_i, \hat{y}_i)$  denotes the loss function, which is typically defined as  $(y_i - \hat{y}_i)^2$ .  $\Omega(f_k)$  is the regularization term used to control model complexity, expressed as:

$$\Omega(f_k) = \gamma T + \frac{1}{2} \lambda \sum_{j=1}^T w_j^2 \quad (6)$$

In this equation,  $T$  is the number of leaves in the tree,  $w_j$  represents the weight of each leaf, and  $\gamma$  and  $\lambda$  are the regularization parameters that control the number of leaves and the magnitude of leaf weights, respectively. The final prediction in XGBoost is obtained by aggregating the predictions from all trees:

$$\hat{y}_i = \sum_{k=1}^K f_k(x_i) \quad (7)$$

where  $\hat{y}_i$  denotes the overall predicted value for sample  $i$ ,  $f_k(x_i)$  represents the prediction of the  $k$ -th tree, and  $K$  is the total number of trees in the ensemble.

## 2.3 Optimization Algorithms

ML models include numerous hyperparameters that significantly influence their predictive performance and generalization capability. In this stage, three metaheuristic optimization algorithms including Ant Colony Optimization (ACO), Particle Swarm Optimization (PSO), and Genetic Algorithm (GA) were employed to fine-tune the model parameters. The subsequent sections provide a detailed description of the working principles of each algorithm and their specific application in hyperparameter optimization. The choice of optimization algorithms was guided by their complementary strengths in exploring complex search spaces. Ant Colony Optimization (ACO) offers strong global search capability and convergence stability, Particle Swarm Optimization (PSO) provides fast convergence and efficient parameter tuning, and the Genetic Algorithm (GA) ensures robust exploration through evolutionary diversity. These characteristics make them particularly suitable for optimizing hyperparameters of nonlinear ML models where conventional grid search methods often fall short in efficiency and accuracy.

### 2.3.1 Ant Colony Optimization (ACO)

Ant Colony Optimization (ACO) is a population-based metaheuristic inspired by the foraging behavior of real ants, which deposit pheromone trails to communicate and collectively identify short or high-quality paths (Dorigo et al., 2007). In this implementation, an artificial ant  $k$  selects to move from node  $i$  to node  $j$  with probability,

$$P_{ij}^k = \frac{[\tau_{ij}]^\alpha \cdot [\eta_{ij}]^\beta}{\sum_{l \in N_i^k} [\tau_{il}]^\alpha \cdot [\eta_{il}]^\beta} \quad (8)$$

where  $\tau_{ij}$  denotes the pheromone concentration on edge  $i-j$ ,  $\eta_{ij}$  is the heuristic desirability (commonly set to  $1/d_{ij}$  when  $d_{ij}$  is a path length or a cost measure), and  $N_i^{(k)}$  is the feasible neighborhood of node  $i$  for ant  $k$ . The parameters  $\alpha$  and  $\beta$  control the relative influence of pheromone intensity and heuristic information, respectively.

After all ants complete a construction step, pheromone trails are updated by applying evaporation and deposition. The pheromone update rule used here is:

$$\tau_{ij}(t+1) = (1 - \rho) \tau_{ij}(t) + \sum_{k=1}^m \Delta\tau_{ij}^{(k)}(t) \quad (9)$$

where  $t$  denotes the iteration index,  $\rho \in (0,1]$  is the pheromone evaporation rate,  $m$  is the number of ants, and  $\Delta\tau_{ij}^{(k)}$  is the amount of pheromone deposited on edge  $i-j$  by ant  $k$  during iteration  $t$ .

### 2.3.2 Particle Swarm Optimization (PSO)

Particle Swarm Optimization (PSO) is a population-based optimization algorithm inspired by the collective movement of birds and fish during food searching (Eberhart and Kennedy, 1995; Pordel and Aminzadeh Ghavifekr, 2024). In this algorithm, each particle represents a potential solution within the search space. The position vector ( $\mathbf{x}_i$ ) and velocity vector ( $\mathbf{v}_i$ ) of each particle are randomly initialized for all dimensions within the predefined parameter bounds, as shown in Eq. (10):

$$\begin{aligned} x_i &= \text{random}(x_{min}, x_{max}) \\ v_i &= \text{random}(v_{min}, v_{max}) \end{aligned} \quad (10)$$

Each particle updates its velocity and position iteratively according to Eq. (11):

$$\begin{aligned} v_i(t+1) &= w \cdot v_i(t) \\ &\quad + c_1 \cdot r_1 \cdot (pbest_i - x_i(t)) \\ &\quad + c_2 \cdot r_2 \cdot (gbest - x_i(t)) \\ x_i(t+1) &= x_i(t) + v_i(t+1) \end{aligned} \quad (11)$$

where  $w$  denotes the inertia weight that balances global exploration and local exploitation,  $c_1$  and  $c_2$  are the cognitive and social learning coefficients, and  $r_1$  and  $r_2$  are random numbers uniformly distributed in  $[0,1]$ . The personal best position ( $pbest_i$ ) and the global best position ( $gbest$ ) are continuously updated based on fitness evaluations until the algorithm converges to an optimal or near-optimal solution.

### 2.3.3 Genetic Algorithm (GA)

The Genetic Algorithm (GA) was employed as a metaheuristic optimization technique to fine-tune the hyperparameters of ML models. Inspired by the Darwinian principles of natural evolution, GA evolves a population of candidate solutions, known as chromosomes, toward optimal configurations. Each chromosome encodes a set of model hyperparameters, and the algorithm iteratively refines them to maximize prediction accuracy and minimize model error (Ranjbar et al., 2022).

Each chromosome is composed of multiple genes, each corresponding to a specific hyperparameter. The initial population is randomly generated within predefined parameter ranges. The population size, which influences both exploration capability and computational cost, is determined according to the dataset size and available computational resources.

The fitness of each chromosome is assessed based on model performance, and the probability of selection is computed using Eq. (12):

$$P(x_i) = \frac{f(x_i)}{\sum_{j=1}^n f(x_j)} \quad (12)$$

where  $n$  is the total population size and  $f(x_i)$  denotes the fitness of chromosome  $i$ . Selected parent chromosomes are combined via a crossover operator to produce offspring, as shown in Eq. (13):

$$\begin{aligned} Child_1 &= \alpha \cdot Parent_1 \\ &\quad + (1 - \alpha) \cdot Parent_2 \\ Child_2 &= \alpha \cdot Parent_2 \\ &\quad + (1 - \alpha) \cdot Parent_1 \end{aligned} \quad (13)$$

where  $\alpha$  is a random crossover coefficient in  $[0,1]$ . To maintain diversity and prevent premature convergence, a mutation operator is applied according to Eq. (14):

$$\hat{x}_i = x_i + random(-\delta, \delta) \quad (14)$$

where  $\delta$  denotes the mutation magnitude. After performing selection, crossover, and mutation, a new generation of chromosomes is formed. The elitism strategy is employed to ensure that the best-performing chromosomes from the previous generation are preserved, guaranteeing that high-quality solutions are not lost.

#### 2.4 Analytical Framework and Model Optimization Process

To improve the predictive accuracy and efficiency of unconfined compressive strength (UCS) estimation for clay soils stabilized with fly ash and blast furnace slag, a hybrid ML–metaheuristic framework was developed. The dataset, consisting of experimentally measured UCS values and corresponding mix design variables, was preprocessed through normalization and outlier screening to ensure statistical consistency. For this purpose, the input variables were normalized using Z-score standardization (Standard Scaler). In this method, each feature is transformed by

subtracting its mean and dividing by its standard deviation:

$$x' = \frac{x - \mu}{\sigma} \quad (15)$$

where  $\mu$  and  $\sigma$  denote the mean and standard deviation of each feature, respectively.

This normalization approach ensures that all input variables contribute equally to the learning process and prevents features with larger magnitudes from dominating the optimization.

Four supervised learning algorithms including ANN, SVM, DT, and XGBoost were trained to capture the nonlinear relationships between input parameters and UCS.

The analytical workflow (summarized in Table 3) defined systematic search ranges for each model's hyperparameters, ensuring an unbiased and comprehensive exploration of parameter space. To enhance model generalization, three bio-inspired optimization algorithms including GA, PSO, and ACO were employed to fine-tune the model parameters (parameter settings summarized in Table 4). In this study, 5-fold cross-validation was applied exclusively to the training dataset during hyperparameter optimization, while an independent test set was reserved for final performance evaluation using  $R^2$ , RMSE, and MAE metrics.

The optimized hyperparameters for all model–optimizer combinations are presented in Table 5, highlighting the relative advantages of each hybrid configuration. All analyses were conducted in Python using Scikit-learn and XGBoost libraries with parallel computation enabled for efficiency. The workflow provides a transparent, reproducible, and statistically rigorous basis for UCS prediction in stabilized

clay soils, supporting data-driven design in geotechnical engineering applications.

**Table 3.** Hyperparameter search ranges of ML models.

ML Model	Parameter	Range
ANN	hidden_layer_sizes	(3, 15)
	number of hidden layers	(1,2)
	transfer function	(relu, tanh, logistic)
	learning_rate_init	(0.0001, 0.1)
SVM	C	(0.1, 100)
	epsilon	(0.01, 1)
DT	max_depth	(2, 20)
	min_samples_split	(2, 20)
XGBoost	n_estimators	(50, 500)
	max_depth	(3, 10)
	learning_rate	(0.01, 0.3)

**Table 4.** Parameters of optimization algorithms.

Algorithm	Parameter	Value
ACO	$\alpha$ (alpha)	1
	$\beta$ (beta)	2
	$\rho$ (rho)	0.5
	q	1
	n_ants	20
	n_iterations	50
PSO	w	0.5
	c <sub>1</sub>	1.5
	c <sub>2</sub>	1.5
	n_particles	20
GA	n_iterations	50
	mutation rate	0.1
	n_population	20
	n_iterations	50

q: pheromone constant, amount deposited by each ant in ACO.

## 2.5 Evaluation metrics

Three metrics were used to evaluate the predictive performance of the ML models for unconfined compressive strength (UCS): the coefficient of determination ( $R^2$ ), mean absolute error (MAE), and root mean square error (RMSE).

The coefficient of determination  $R^2$  quantifies the proportion of variance in the observed data explained by the model. It can be computed from residual and total sum of squares as:

$$R^2 = 1 - \frac{\sum_{i=1}^N (y_i - \hat{y}_i)^2}{\sum_{i=1}^N (y_i - \bar{y})^2} \quad (16)$$

where  $N$  is the number of samples,  $y_i$  the observed (actual) value,  $\hat{y}_i$  the predicted value, and  $\bar{y} = \frac{1}{N} \sum_{i=1}^N y_i$  the sample mean of observed values. Values of  $R^2$  closer to 1 indicate better fit.

Mean absolute error (MAE) measures the average magnitude of prediction errors in the same units as the target:

$$MAE = \frac{1}{N} |\hat{y}_i - y_i| \quad (17)$$

MAE is robust to outliers relative to RMSE and is easy to interpret because it has the same unit as the predicted quantity.

Root mean square error (RMSE) penalizes larger errors more strongly and is defined as:

$$RMSE = \sqrt{\frac{1}{N} \left( \sum_{i=1}^N (\hat{y}_i - y_i)^2 \right)} \quad (18)$$

Lower values of MAE and RMSE indicate better predictive accuracy; RMSE is more sensitive to large deviations (outliers) due to the squaring of errors.

## 3 Results and Discussion

The developed hybrid modeling framework successfully established predictive relationships between mix design parameters and the unconfined compressive strength (UCS) of stabilized clay soils. The integration of ML models with population-based optimization algorithms significantly improved predictive reliability and reduced variance across repeated runs.

**Table 5.** Optimized hyperparameters of ML models.

ANN			
Parameter	ACO	GA	PSO
Activation function	tanh	logistic	tanh
Number of hidden layers	2	2	2
n <sub>1</sub>	15	15	15
n <sub>2</sub>	15	15	15
learning rate	0.0756	0.0220	0.0544
DT			
Parameter	ACO	GA	PSO
max depth	20	11	11
min samples split	2.48	3.96	3.53
SVM			
Parameter	ACO	GA	PSO
C	71.21	75.21	69.97
ε (epsilon)	0.4052	0.1839	0.2117
XGBoost			
Parameter	ACO	GA	PSO
n estimators	266	97	209
learning rate	0.1319	0.1330	0.1319
max depth	7	7	7

Optimization procedures converged smoothly for all algorithm–model combinations, with convergence typically achieved within 30 to 40 iterations out of the 50 total.

### 3.1 Comparative Performance of ML Models

Figure 2 clearly illustrates that the ANN-PSO and ANN-GA models delivered the highest predictive accuracy, with  $R^2$  values of 0.98 and 0.977, respectively, while the XGBoost-GA model followed closely ( $R^2 = 0.975$ ). The decision tree and SVM models, although less complex, achieved moderate yet consistent performance, reflecting their limited ability to capture nonlinear patterns. Overall, the scatterplots in Figure 2 reveal a strong alignment between predicted and measured UCS values, as most data points lie close to the 1:1 reference line, demonstrating the effectiveness and robustness of the hybrid optimization strategy.

Figure 3 demonstrates that the ANN models consistently outperformed other learners in terms of predictive accuracy and stability across all optimization

algorithms. The ANN-PSO model yielded the lowest root mean square error (RMSE=0.88 MPa) and mean absolute error (MAE=0.62 MPa), confirming its superior ability to capture nonlinear effects of fly ash and slag proportions on UCS. The XGBoost models ranked second in overall performance, providing a strong balance between bias and variance, while maintaining relatively faster training convergence. In contrast, the SVM and DT models exhibited higher RMSE values (1.10–1.25 MPa) and lower  $R^2$  ( $\approx 0.96$ – $0.97$ ), suggesting limited adaptability to complex interaction terms within the input space. These results indicate that deeper model architectures and ensemble-based learners, particularly those with adaptive optimization, are better suited for representing the nonlinear strength development behavior of stabilized clay systems.

### 3.2 Influence of Metaheuristic Optimization Algorithms

The influence of metaheuristic optimization algorithms on model performance was evaluated using the

optimized hyperparameters summarized in Table 5 and the comparative results shown in Figure 3. As illustrated, PSO generally achieved the highest predictive accuracy across most machine learning models, followed by GA and ACO. This behavior can be attributed to PSO's velocity-based update mechanism, which enables an effective balance between global exploration and local exploitation of the hyperparameter space. The optimized results indicate that, while all optimizers converged to similar ANN architectures, PSO selected relatively higher learning rates, whereas ACO favored more conservative values, leading to more stable but slightly less accurate solutions. In the DT and SVM models, PSO and GA tended to produce more regularized configurations compared to ACO, contributing to improved generalization. For XGBoost, all optimizers converged to identical tree depths, although differences in the number of estimators reflected distinct search behaviors.

Overall, the results confirm that optimizer selection significantly affects both convergence characteristics and predictive accuracy, highlighting the importance of metaheuristic choice in hybrid ML modeling.

Table 6 provides important insight into the generalization behavior of the developed hybrid models by comparing training and testing  $R^2$  values across all model-optimizer combinations. The consistently high  $R^2$  values obtained for both training and testing datasets indicate that the optimized models

successfully learned the underlying nonlinear relationships without overfitting. Notably, the relatively small gap between training and testing  $R^2$  values for ANN-based models confirms their strong generalization capability, which is essential for reliable UCS prediction in practical applications. The slight reduction in test  $R^2$  compared to training values reflects realistic performance degradation when models are exposed to unseen data, reinforcing the credibility of the modeling framework. Furthermore, the stability of  $R^2$  across different optimizers suggests that the dataset contains sufficient information to support robust learning. These results collectively demonstrate that the hybrid optimization strategy enhances predictive accuracy while maintaining model reliability and transferability.

Figure 4 illustrates the convergence behavior of the optimized ANN-PSO model, displaying a rapid error reduction within the initial 15 epochs followed by a stable asymptotic phase. The close alignment between training and testing curves confirms the model's strong generalization capability and absence of overfitting. This efficient convergence highlights PSO's ability to effectively balance global exploration with local exploitation. Furthermore, to ensure computational transparency, a detailed step-by-step calculation of a representative sample using the extracted weights and biases is provided in Appendix A.

**Table 6.**  $R^2$  values of train and test data.

Model	ANN			DT			SVM			XGBOOST		
	ACO	GA	PSO	ACO	GA	PSO	ACO	GA	PSO	ACO	GA	PSO
$R^2_{\text{Train}}$	0.993	0.982	0.998	0.998	0.998	0.998	0.981	0.981	0.981	1.000	0.998	1.000
$R^2_{\text{Test}}$	0.970	0.977	0.980	0.969	0.969	0.969	0.963	0.960	0.960	0.974	0.975	0.974

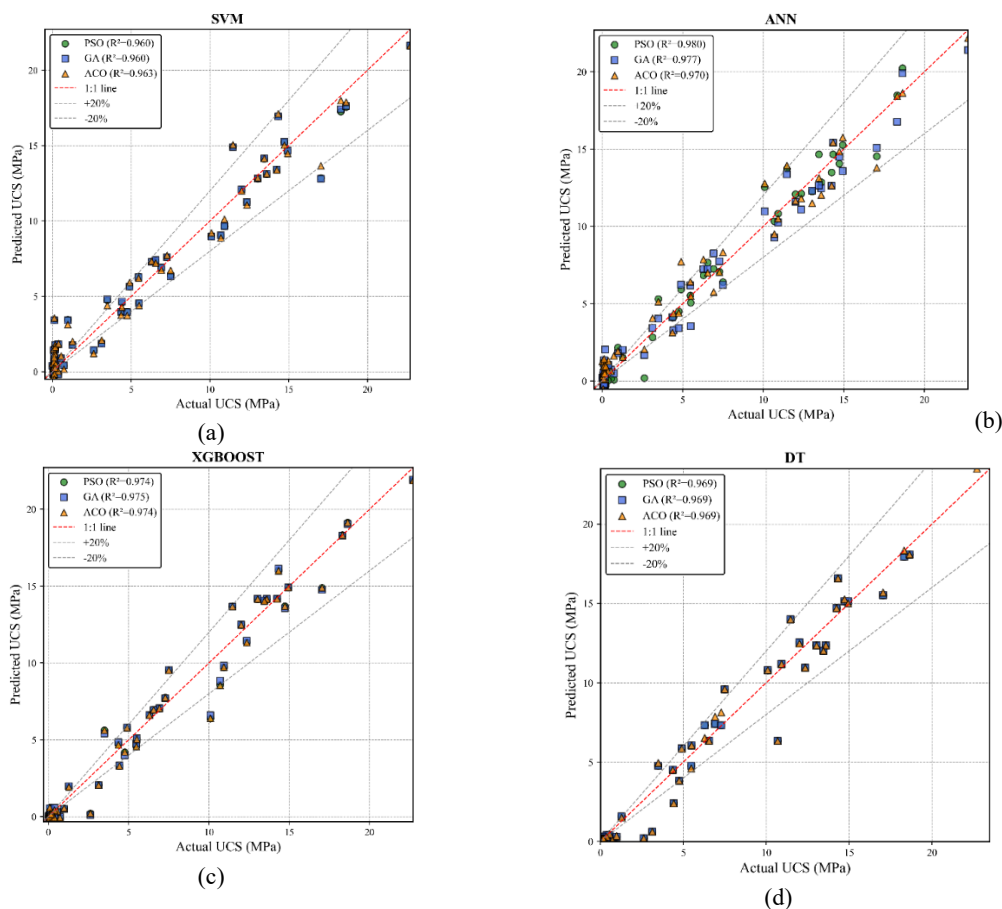


**Figure 2.** Comparison of the predicted and actual UCS values for different ML models during the testing phase: (a) SVM, (b) ANN, (c) XGBoost, (d) DT.

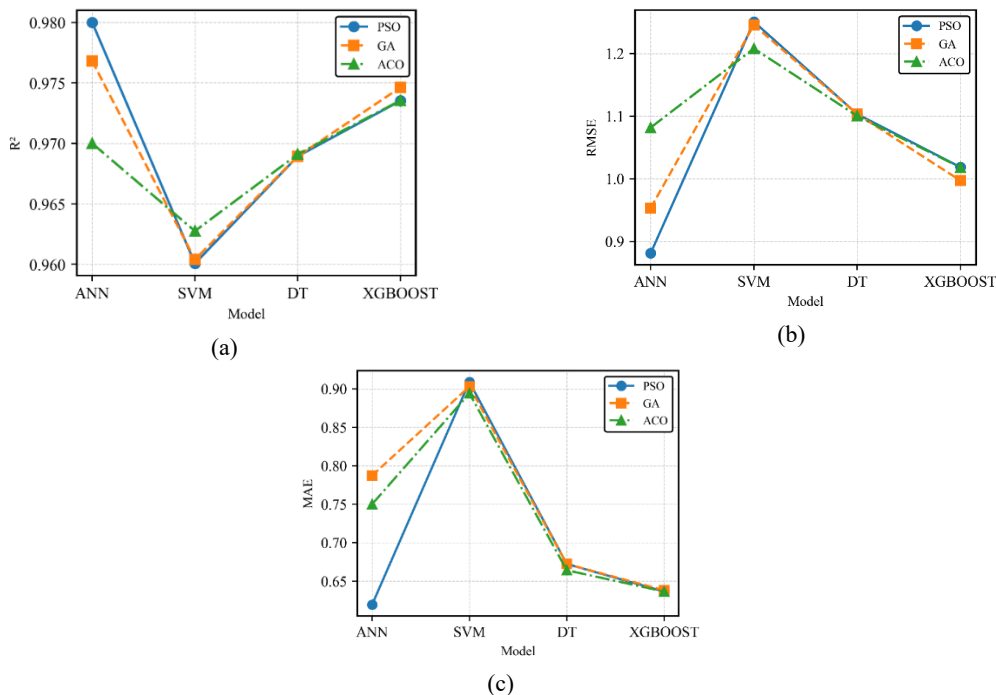


**Figure 3.** Performance evaluation metrics of different ML models optimized by metaheuristic algorithms (a) R2 (b) RMSE (c) MAE.

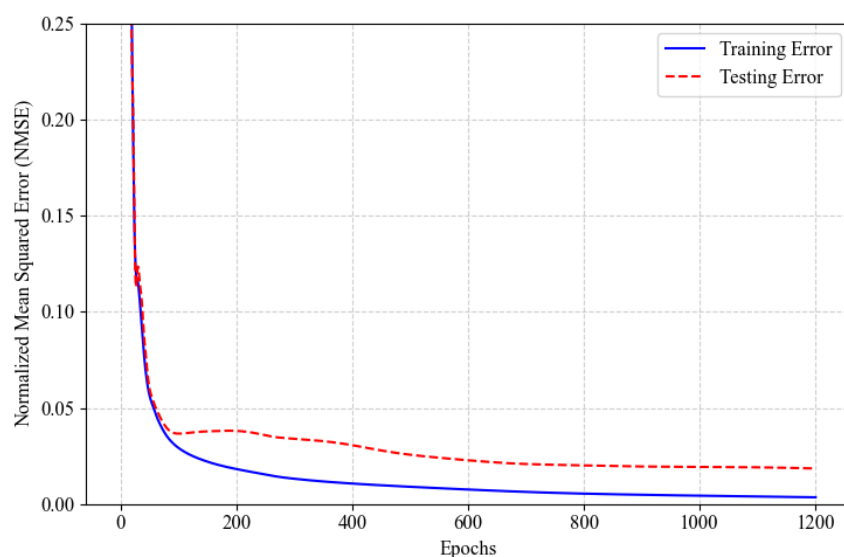


**Figure 4.** Evolution of training and testing errors for the optimized ANN-PSO model.

### 3.3 Comparison with previous studies

In this study, the combined ANN-PSO model performed very well in predicting the compressive strength of stabilized soil, achieving a coefficient of determination of  $R^2=0.98$ . This value is significantly improved compared to linear models. For example, in the study of Mozumder and Laskar (2015), which used multivariate regression, the value of  $R^2=0.899$  was reported, indicating the limited accuracy of this approach. In the study of Javdanian and Lee (2019), using the group method of data handling (GMDH) model together with the PSO algorithm increased the accuracy and achieved  $R^2=0.953$ ; however, this value was still lower than the results of the present model. Subsequently, more recent studies using more advanced methods such as Random Forest ( $R^2=0.976$ : Zeini et al., 2023) and AdaBoost algorithm ( $R^2=0.975$ : Abdullah et al., 2024) improved the estimation accuracy compared to previous models. It should be noted that although the same source of experimental data was used, the exact training-testing splits employed in

previous studies were not available; therefore, the comparisons are intended to be indicative of relative predictive performance rather than a direct one-to-one evaluation.

Despite these improvements, the results of the present study show that the combination of ANN with the PSO metaheuristic algorithm has been able to improve the prediction accuracy more than previous studies by optimally adjusting the hyperparameters and reducing the error. This improvement not only indicates the technical superiority of the proposed model, but also shows that combined approaches based on ML and optimization can be used as reliable tools for the design and analysis of stabilized soils in geotechnical engineering.

### 3.4 Sensitivity Analysis

In order to investigate the effect of various parameters on the compressive strength of stabilized soil, sensitivity analysis was performed using the cosine domain method. This method, introduced by Heidari and Ghanizadeh (2020), is used to determine the relative

importance of each input variable in the prediction model. In this method, the influence of each variable on the compressive strength is determined by calculating the correlation between each input variable and the output variable:

$$R_i = \frac{\sum_{k=1}^m x_{ik}y_k}{\sqrt{\sum_{k=1}^m x_{ik}^2 \times \sum_{k=1}^m y_k^2}} \quad (19)$$

where  $R_i$  is the sensitivity coefficient representing the relative importance of the  $i$ th input variable.  $x_{ik}$  is the value of the  $i$ th input variable and  $y_k$  is the target parameter (UCS) in the  $k$ th experiment.  $m$  is also equal to the total number of experiments. The larger value in this relation indicates a greater effect of that feature on the target parameter. The value of  $R_i$  varies between 0 and 1; so that values close to 1 indicate a very large effect of that variable on the compressive strength and values close to zero indicate a negligible effect of that variable. Given that the XGBoost model in combination with different algorithms provided the best estimate of the soil

resistance, its results were used to perform a sensitivity analysis (Figure 5). The sensitivity analysis showed that among the stabilization factors studied, blast furnace slag with  $R_i= 0.87$  has the greatest effect on increasing the uniaxial compressive strength of the soil. Parameters related to alkaline activators also play a significant role in this increase in resistance. However, the results indicate that fly ash with  $R_i= 0.06$  did not have much effect on the soil stabilization process in this study. This may be related to the incompatibility of this type of activator or soil with the geopolymerization process of fly ash. In addition, the sensitivity analysis showed that the response of different soil types to the stabilization process is different. For example, soil type 3 with  $R_i= 0.57$  showed a better response than soil type 1 with  $R_i= 0.18$ . This finding allows the selection of appropriate stabilization methods for each soil type and helps geotechnical engineers to make optimal decisions according to the unique characteristics of each soil.

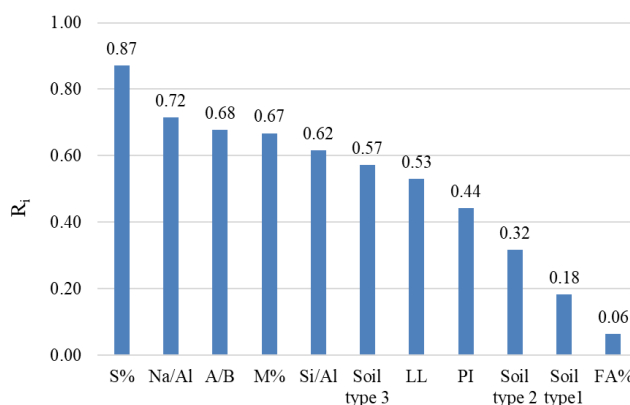


Figure 5. Comparison of the effects of different input parameters on the predicted UCS values.

### 3.5 Parametric Analysis

The parametric analysis presented in Figure 6 clarifies the physical impact of input variables on UCS development in geopolymer-stabilized clay soils. The

results indicate that binder-related parameters, particularly blast furnace slag content, exert a dominant influence on strength enhancement, reflecting the critical role of calcium-rich phases in

promoting geopolymer gel formation. In contrast, fly ash content exhibits a comparatively weaker effect, suggesting its low reactivity under the specific ambient curing conditions employed in this study. Furthermore, chemical ratios such as Si/Al and Na/Al display pronounced non-linear trends, highlighting the existence of optimal chemical balances essential for network formation. Variations in molarity and alkaline-to-binder (A/B) ratio

demonstrate that excessive activator concentrations do not yield proportional strength gains; instead, they may hinder geopolymerization due to chemical saturation or ionic imbalance. These observations confirm that UCS development is governed by complex interactions effectively captured by the optimized ANN framework, providing practical guidance for mix design optimization.

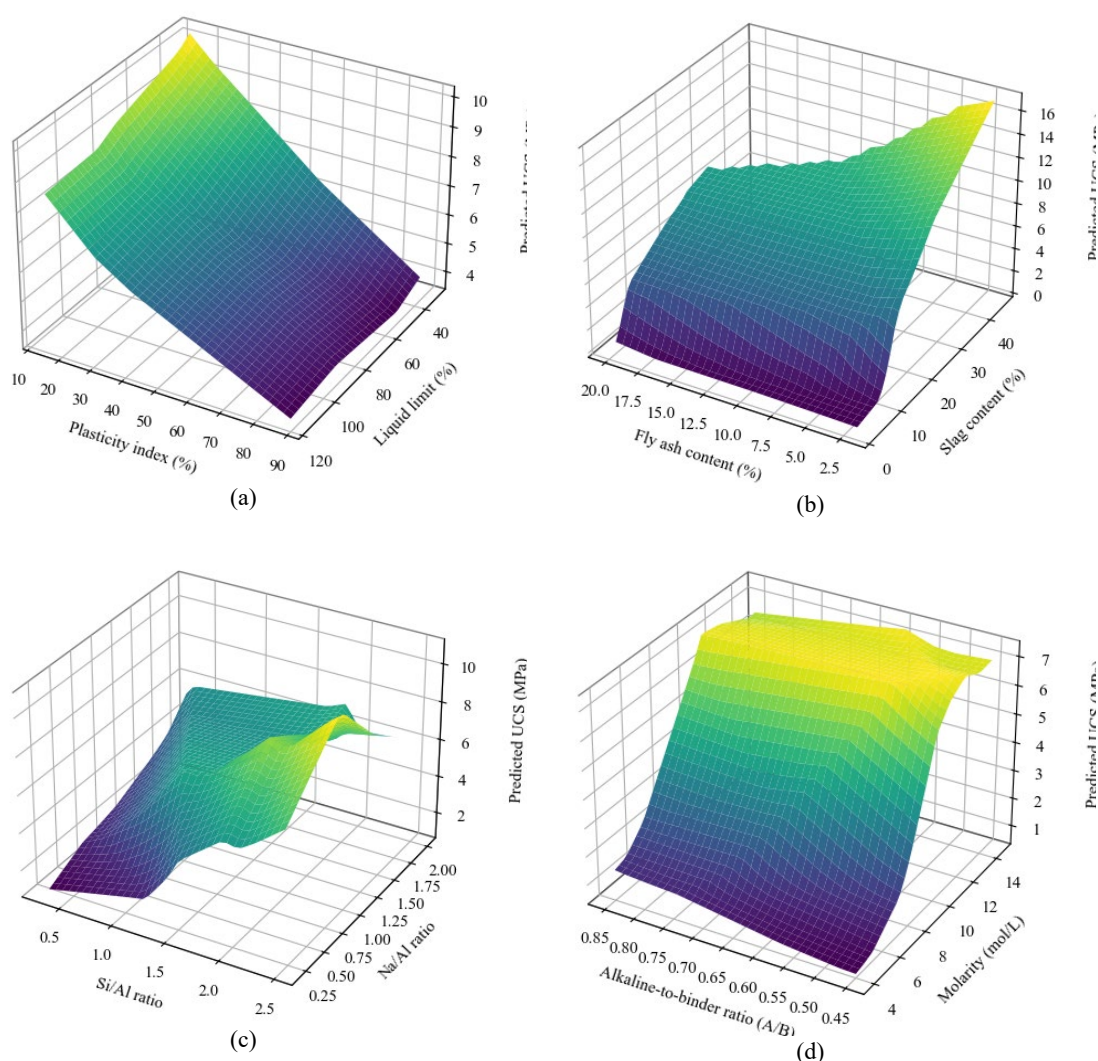


**Figure 6.** Parametric analysis illustrating the influence of (a) LL and PI (b) slag and fly ash (c) Si/Al and Na/Al (d) molarity and A/B on UCS.

#### 4 Conclusions

This study developed and validated a hybrid ML framework integrated with metaheuristic optimization algorithms to accurately predict the unconfined compressive strength (UCS) of geopolymer-stabilized clay soils. Among the various model–optimizer combinations tested, the ANN-PSO achieved the highest predictive accuracy ( $R^2 \approx 0.98$ ), followed closely by and ANN-GA ( $R^2 \approx 0.977$ ), outperforming other configurations such as XGBoost-GA and traditional linear or regression-based models. The hybrid approach effectively captured the complex nonlinear interactions between material composition, curing conditions, and activator concentrations; relationships that conventional methods often fail to model. Sensitivity analysis further revealed that blast furnace slag content exerted the most significant influence on UCS, followed by parameters related to activator molarity and soil type, providing valuable insight into the material behavior governing strength development. The parametric analysis also confirmed the strong influence of material composition and activator-related parameters on strength development. Variations in slag content, alkaline activator molarity, and Na/Al and Si/Al ratios produced pronounced and nonlinear effects on UCS, whereas fly ash exhibited a comparatively limited contribution within the investigated range.

The findings of this study have meaningful implications for both research and practice in geotechnical engineering. By integrating advanced learning algorithms with bio-inspired optimization methods, this framework provides a fast, data-driven alternative to conventional experimental testing. The

developed models can serve as reliable tools for predicting UCS in soil stabilization projects, minimizing the need for extensive laboratory work while improving the precision of mix design. In practical applications, the approach can support decision-making in sustainable infrastructure development, particularly in optimizing the use of industrial by-products such as fly ash and slag to reduce environmental impact. Furthermore, the hybrid modeling strategy can be extended to other geotechnical problems, including shear strength estimation, settlement prediction, and durability assessment of stabilized soils under various environmental conditions.

Future research should focus on expanding the dataset with a wider range of soil types and binder combinations to enhance the generalizability of the models. Incorporating microstructural and mineralogical data could also improve the interpretability of the ML predictions and strengthen the connection between physical mechanisms and computational outcomes. Additionally, integrating uncertainty quantification methods and explainable AI frameworks would provide deeper insights into model reliability and feature interactions. Real-world validation through field projects and the creation of practical, engineer-oriented software based on these hybrid models would turn this research from theory into action. These tools could make it easier for designers to apply data-driven methods for stronger, more sustainable soil stabilization. Moreover, the developed ANN–PSO model can be readily implemented in geotechnical design workflows or pavement design software to provide rapid, preliminary UCS predictions based on easily

measurable input parameters. This practical integration bridges the gap between laboratory research and real-world geotechnical engineering applications.

It should be noted that the dataset includes only three soil types, which may restrict the generalizability of the developed machine learning models to broader geotechnical conditions. Although the proposed frameworks demonstrated strong predictive performance, their applicability to soils with different mineralogical compositions, gradations, and plasticity characteristics requires further validation. Future studies should incorporate more diverse soil types, larger datasets, and multi-source experimental data. In addition, extending the analysis to field-scale conditions and exploring parameter-free optimization algorithms would further enhance model robustness and practical relevance.

## References

- Abdullah, G. M., Ahmad, M., Babur, M., Badshah, M. U., Al-Mansob, R. A., Gamil, Y., & Fawad, M. (2024). Boosting-based ensemble machine learning models for predicting unconfined compressive strength of geopolymer stabilized clayey soil. *Scientific Reports*, 14(1), 2323.
- Eberhart, R., & Kennedy, J. (1995). Particle swarm optimization. *Proceedings of the IEEE international conference on neural networks*, 69-73.
- Behnood, A. (2018). Soil and clay stabilization with calcium- and non-calcium-based additives: A state-of-the-art review of challenges, approaches and techniques. *Transportation Geotechnics*, 17, 14–32. <https://doi.org/10.1016/j.trgeo.2018.08.002>
- Das, S. K., Samui, P., & Sabat, A. K. (2011). Application of artificial intelligence to maximum dry density and unconfined compressive strength of cement stabilized soil. *Geotechnical and Geological Engineering*, 29(3), 329–342.
- de Araújo, M. T., Ferrazzo, S. T., Chaves, H. M., da Rocha, C. G., & Consoli, N. C. (2023). Mechanical behavior, mineralogy, and microstructure of alkali-activated wastes-based binder for a clayey soil stabilization. *Construction and Building Materials*, 362, 129757.
- Dhaliwal, S. S., Nahid, A.-A., & Abbas, R. (2018). Effective intrusion detection system using XGBoost. *Information*, 9, 149.
- Dorigo, M., Birattari, M., & Stutzle, T. (2007). Ant colony optimization. *IEEE computational intelligence magazine*, 1(4), 28-39.
- Ghadir, P., & Ranjbar, N. (2018). Clayey soil stabilization using geopolymer and Portland cement. *Construction and Building Materials*, 188, 361–371.
- Ghanizadeh, A. R., & Naseralavi, S. S. (2023). Intelligent prediction of unconfined compressive strength and Young's modulus of lean clay stabilized with iron ore mine tailings and hydrated lime using Gaussian process regression. *Journal of Soft Computing in Civil Engineering*, 7(4).
- Ghanizadeh, A. R., & Safi Jahanshahi, F. (2024). Intelligent Modeling of Unconfined Compressive Strength of Stabilized Clay Soil using Gene Expression Programming. *Road*, 32(119), 137-156. <https://doi.org/10.22034/road.2023.399936.2>
- Ghanizadeh, A. R., Heidarabadizadeh, N., Bayat, M., & Khalifeh, V. (2022). Modeling of unconfined compressive strength and Young's modulus of lime and cement stabilized clayey subgrade soil using evolutionary polynomial regression (EPR). *International Journal of Mining and Geo-Engineering*. <https://doi.org/10.22059/IJMGE.2022.306688.594858>
- Ghanizadeh, A. R., Safi Jahanshahi, F., & Naseralavi, S. S. (2024). Intelligent modelling of unconfined compressive strength of cement stabilised iron ore tailings: a case study of Golgohar mine. *European Journal of Environmental and Civil Engineering*, 28(8), 1759-1787.
- Ghanizadeh, A. R., Safi Jahanshahi, F., & Ziayi, A. (2025). Presenting a Model for Predicting CBR and UCS of Expensive Soil Stabilized with Hydrated Lime Activated with Rice Husk Ash Using the Hybrid MARS-EBS Method. *Road*, 33(122), 45-66.

- <https://doi.org/10.22034/road.2024.431647.2>  
231
- Güllü, H. (2014). Function finding via genetic expression programming for strength and elastic properties of clay treated with bottom ash. *Engineering Applications of Artificial Intelligence*, 35, 143–157.
- Heidari Dezfuli, T., & Ghanizadeh, A. R. (2020). Prediction of compressive and tensile strength of clayey subgrade soil stabilized with Portland cement and iron ore mine tailing using computational intelligence methods. *Civil Infrastructure Researches*, 6(1), 73–88.
- Hoy, M., Horpibulsuk, S., & Arulrajah, A. (2016). Strength development of recycled asphalt pavement–fly ash geopolymer as a road construction material. *Construction and Building Materials*, 117, 209–219. <https://doi.org/10.1016/j.conbuildmat.2016.04.136>
- Javdanian, H., & Lee, S. (2019). Evaluating unconfined compressive strength of cohesive soils stabilized with geopolymer: A computational intelligence approach. *Engineering with Computers*, 35(1), 191–199.
- Johari, A., Golkarfard, H., Davoudi, F., & Fazeli, A. (2021). A predictive model based on the experimental investigation of collapsible soil treatment using nano-clay in the Sivand Dam region, Iran. *Bulletin of Engineering Geology and the Environment*, 80(9), 6725–6748.
- Johari, A., Golkarfard, H., Davoudi, F., & Fazeli, A. (2022). Experimental investigation of collapsible soils treatment using nano-silica in the Sivand Dam Region, Iran. *Iranian Journal of Science and Technology, Transactions of Civil Engineering*, 46(2), 1301–1310.
- Johari, A., Javadi, A., & Habibagahi, G. (2011). Modelling the mechanical behaviour of unsaturated soils using a genetic algorithm-based neural network. *Computers and Geotechnics*, 38(1), 2–13.
- Mahmoodi, K., & Momeni, H. (2024). Comparison of various machine learning algorithms for estimation of uniaxial compressive strength of cement and volcanic ash stabilized clay. *Iranian Journal of Geophysics*, 18(2), 19–37. (In Persian).
- Mahmoodi, K., Mahbubi Motlagh, N., & Mahboubi Ardakani, A.-R. (2024). An investigation into the effects of lime-stabilization on soil–geosynthetic interface behavior. *Geomechanics and Engineering*, 38(3), 231.
- Miao, S., Shen, Z., Wang, X., Luo, F., Huang, X., & Wei, C. (2017). Stabilization of highly expansive black cotton soils by means of geopolymerization. *Journal of Materials in Civil Engineering*, 29(10), 04017170.
- Mozumder, R. A., & Laskar, A. I. (2015). Prediction of unconfined compressive strength of geopolymer stabilized clayey soil using artificial neural network. *Computers and Geotechnics*, 69, 291–300.
- Mozumder, R. A., Laskar, A. I., & Hussain, M. (2017). Empirical approach for strength prediction of geopolymer stabilized clayey soil using support vector machines. *Construction and Building Materials*, 132, 412–424.
- Pordel, M., & Aminzadeh Ghavifekr, A. (2024). Analysis of factors influencing concrete resistance in construction industry: Machine learning approach. *Journal of Civil and Environmental Engineering*.
- Ranjbar, I., Toufigh, V., & Boroushaki, M. (2022). A combination of deep learning and genetic algorithm for predicting the compressive strength of high-performance concrete. *Structural Concrete*, 23(4), 2405–2418.
- Raschka, S., Liu, Y. H., & Mirjalili, V. (2022). *Machine learning with PyTorch and Scikit-Learn*.
- Sukprasert, S., Hoy, M., Horpibulsuk, S., Arulrajah, A., Rashid, A. S. A., & Nazir, R. (2021). Fly ash based geopolymer stabilisation of silty clay/blast furnace slag for subgrade applications. *Road Materials and Pavement Design*, 22(2), 357–371.
- Theobald, O. (2017). *Machine learning for absolute beginners: A plain English introduction* (Vol. 157). Scatterplot Press, London, UK.
- Xue, X., Yang, X., & Chen, X. (2014). Application of a support vector machine for prediction of slope stability. *Science China Technological Sciences*, 57(12), 2379–2386. <https://doi.org/10.1007/s11431-014-5699-6>
- Zeini, H. A., Al-Jeznawi, D., Imran, H., Bernardo, L. F. A., Al-Khafaji, Z., & Ostrowski, K. A. (2023). Random forest algorithm for the strength prediction of geopolymer stabilized clayey soil. *Sustainability*, 15(2), 1408.
- Zhang, W., Wu, C., Zhong, H., Li, Y., & Wang, L. (2021). Prediction of undrained shear strength using

extreme gradient boosting and random forest based on Bayesian optimization. *Geoscience Frontiers*, 12(1), 469-477.  
<https://doi.org/https://doi.org/10.1016/j.gsf.2020.03.007>.